

Evolutionary origin of the turtle skull

G. S. Bever^{1,2,3}, Tyler R. Lyson^{3,4}, Daniel J. Field⁵ & Bhart-Anjan S. Bhullar^{5,6}

Transitional fossils informing the origin of turtles are among the most sought-after discoveries in palaeontology^{1–5}. Despite strong genomic evidence indicating that turtles evolved from within the diapsid radiation (which includes all other living reptiles^{6,7}), evidence of the inferred transformation between an ancestral turtle with an open, diapsid skull to the closed, anapsid condition of modern turtles remains elusive. Here we use high-resolution computed tomography and a novel character/taxon matrix to study the skull of *Eunotosaurus africanus*, a 260-million-year-old fossil reptile from the Karoo Basin of South Africa, whose distinctive postcranial skeleton shares many unique features with the shelled body plan of turtles^{2–4}. Scepticism regarding the status of *Eunotosaurus* as the earliest stem turtle arises from the possibility that these shell-related features are the products of evolutionary convergence. Our phylogenetic analyses indicate strong cranial support for *Eunotosaurus* as a critical transitional form in turtle evolution, thus fortifying a 40-million-year extension to the turtle stem and moving the ecological context of its origin back onto land^{8,9}. Furthermore, we find unexpected evidence that *Eunotosaurus* is a diapsid reptile in the process of becoming secondarily anapsid. This is important because categorizing the skull based on the number of openings in the complex of dermal bone covering the adductor chamber has long held sway in amniote systematics¹⁰, and still represents a common organizational scheme for teaching the evolutionary history of the group. These discoveries allow us to articulate a detailed and testable hypothesis of fenestral closure along the turtle stem. Our results suggest that *Eunotosaurus*

represents a crucially important link in a chain that will eventually lead to consilience in reptile systematics, paving the way for synthetic studies of amniote evolution and development.

At least 270 million years⁶ of evolution within the reptile crown clade has produced a panoply of cranial forms. From the hyperkinetic anatomy of snakes to the encephalized and highly visual architecture of birds, the reptile skull is an increasingly popular model for understanding the evolution and development of vertebrate adaptation^{11,12}. Turtles are an important yet enigmatic piece of this evolutionary puzzle. The earliest uncontroversial stem turtles^{1,13} exhibit an anapsid skull with an adductor chamber concealed by bone (Fig. 1). Although emargination has modified this dermal covering in the vast majority of crown-group turtles¹⁴, the absence of temporal fenestration is a feature shared by currently recognized crown- and stem-group turtles, the immediate fossil outgroups of the amniote crown clade, and many early reptiles (sauropsids)¹⁰. If this absence reflects conservation of the ancestral amniote condition, then turtles are an extant remnant of an early reptile radiation that excludes the other living forms (tuatara, lizards, snakes, crocodilians, birds). If, however, turtles are nested within the radiation of anatomically diapsid reptiles, which includes both the diapsid crown group and a majority of its stem lineage¹⁵, then the anapsid skull of turtles is a secondary configuration built on an ancestrally diapsid structural plan. Despite the strong support that a diapsid origin of turtles enjoys from genomic data sets^{6,7}, no direct palaeontological evidence yet exists for the loss of a diapsid skull along the turtle stem. This situation epitomizes a general discord between the fossil record and the molecular signature of living taxa that

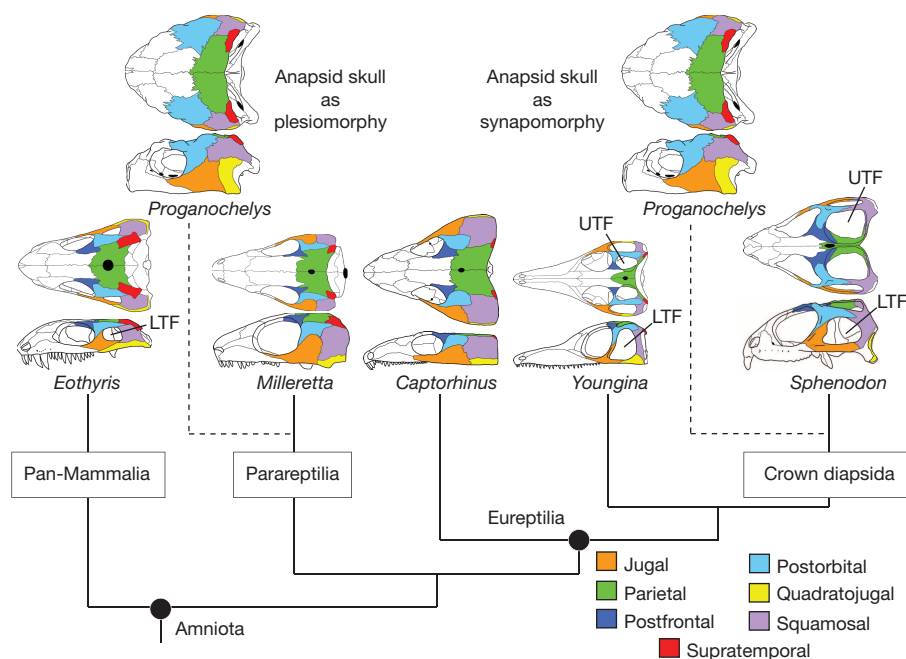


Figure 1 | Competing hypotheses for the origin of the anapsid skull of modern turtles. Historically, this closed condition was accepted as the conservation of the ancestral amniote state with turtles originating among early, long-extinct forms^{10,15}. More recent analyses largely reject this hypothesis for a turtle origin within crown-group Diapsida^{16,17}—a radiation that includes modern lizards, snakes, tuatara, crocodilians, and birds, and that is generally characterized by a skull with upper and lower temporal fenestrae (UTF and LTF, respectively).

¹Department of Anatomy, New York Institute of Technology, College of Osteopathic Medicine, Old Westbury, New York 11568, USA. ²Division of Paleontology, American Museum of Natural History, New York, New York 10024, USA. ³Evolutionary Studies Institute, University of the Witwatersrand, Private Bag 3, P.O. WITS, Johannesburg 2050, South Africa. ⁴Department of Earth Sciences, Denver Museum of Nature and Science, Denver, Colorado 80205, USA. ⁵Department of Geology & Geophysics and Peabody Museum of Natural History, Yale University, New Haven, Connecticut 06520, USA. ⁶Department of Organismal Biology and Anatomy, University of Chicago, Chicago, Illinois 60637, USA.

currently obfuscates attempts to synthesize broad evolutionary patterns across Reptilia¹⁶.

Eunotosaurus africanus Seeley is an approximately 260-million-year-old fossil reptile from South Africa¹⁷ that shares a number of uniquely derived postcranial features with turtles—features that appear to inform the evolutionary origin of the iconic turtle shell and the highly derived mechanism by which turtles ventilate their lungs^{2–4}. The character-rich skull is an obvious source for testing these homology claims, but cranial details for *Eunotosaurus* remain scant. Existing studies stress the lack of cranial support for a privileged *Eunotosaurus*–turtle relationship^{18–20}, thus establishing a cranial–postcranial conflict that parallels the ongoing genotypic–phenotypic phylogenetic dispute. Here we use high-resolution computed tomography and phylogenetic analyses to: (1) examine the skull of *Eunotosaurus*; (2) test the current hypothesis that cranial data do not support this taxon as an early stem turtle; and (3) formulate an evolutionary model (predictive series of evolutionary steps) for the origin of the anapsid skull of modern turtles.

The skull of *Eunotosaurus* is relatively short and wide (Figs 2, 3 and Extended Data Figs 1–3). Its compact snout bears approximately 23 robust, subthecodont marginal teeth and nasals that are longer than the frontals. The palate includes an unfused basicranial articulation, an

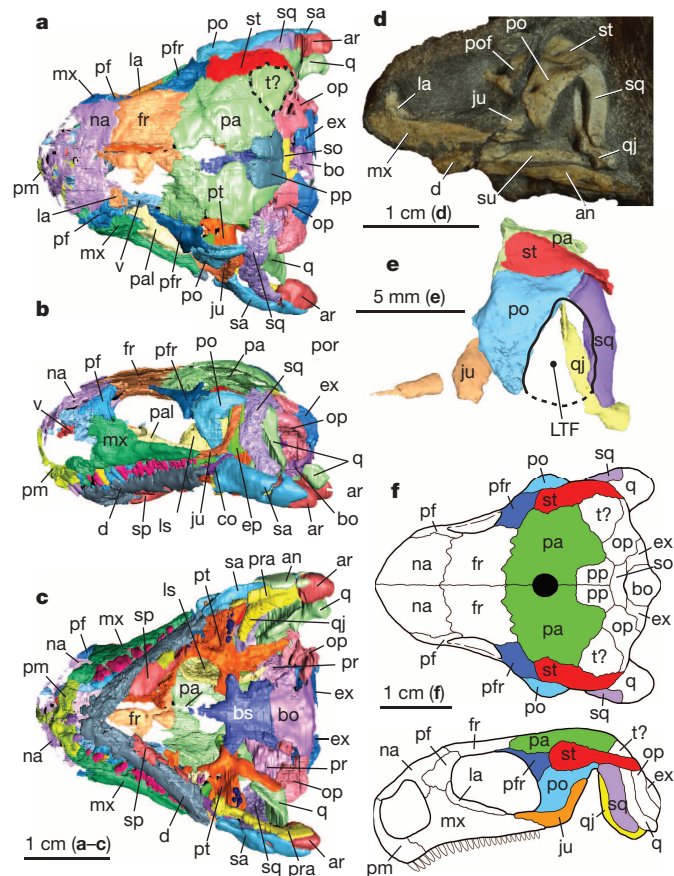


Figure 2 | The adult skull of the early stem turtle *Eunotosaurus africanus*. a–c, Dorsal (a), left lateral (b), and ventral (c) views of the digitally segmented skull of CM777. d, Reflected right lateral view of CM 86–341. e, Digitally rendered and reflected right lateral view of the temporal region of CM 86–341. f, Composite reconstruction of dorsal (top) and left lateral (bottom) views. an, angular; ar, articular; bo, basioccipital; bs, parabasisphenoid; co, coronoid; d, dentary; ep, epipterygoid; ex, exoccipital; fr, frontal; ju, jugal; la, lacrimal; ls, laterosphenoid; mx, maxilla; na, nasal; op, opisthotic; pa, parietal; pra, prearticular; pf, prefrontal; pfr, postfrontal; po, postorbital; pp, postparietal; pr, prootic; pt, pterygoid; q, quadrate; qj, quadratojugal; sa, surangular; so, supraoccipital; sp, splenial; sq, squamosal; st, supratemporal; t?, putative tabular; v, vomer.

absence of basioccipital tubera, a laterally angled transverse process of the pterygoid, an edentulous ectopterygoid, a long interpterygoid vacuity, and a moderately sized suborbital fenestra. The gracile lower jaw exhibits a prominent coronoid process, a surangular that contributes to the articular surface, a splenial that does not participate in the mandibular symphysis, and 18 teeth.

The cheek is open with a single, large fenestra. The fenestra is defined anteriorly by an expanded postorbital and tall, comma-shaped jugal. Its posterior margin is formed by an elongate, vertically oriented squamosal and quadratojugal. The quadratojugal is especially tall, spanning the full height of the cheek. A lower temporal arcade is not present, leaving the cheek open ventrally. The roof of the adductor chamber in a juvenile skull is marked by a distinct upper temporal fenestra (on both sides; Extended Data Fig. 2), previously unrecognized and identical to the unique upper temporal fenestra in uncontroversial diapsid reptiles, which is separated from the lower fenestra by a completed upper temporal arcade (Fig. 3). In the adult, the upper fenestra is covered by a distinctly elongate supratemporal that contacts the postorbital and postfrontal anteriorly (Fig. 2). Digital removal of the supratemporal reveals the upper fenestra is retained in the adult, though its diameter is reduced through expansion of the surrounding elements—most notably the postorbital and squamosal (Fig. 3). The relatively late ontogenetic expansion of these bones also reduces the circumference of the lower temporal fenestra and modifies its rounded shape. The adductor chamber is closed posteriorly by what appears to be an expanded tabular, though this bony plate may represent a posterolateral flange of the parietal. The putative tabular fills a space corresponding to what would otherwise be a moderately sized post-temporal fenestra (Extended Data Fig. 3).

Phylogenetic analyses, employing maximum parsimony and Bayesian optimality criteria were performed on both the complete character matrix and one restricted to cranial features, all of which strongly support an exclusive *Eunotosaurus*–turtle clade (Extended Data Figs 4–7). Examples of turtle features expressed in the skull of *Eunotosaurus* include marked preorbital shortening, relative shortening of the frontals, prootic–quadrate contact, and an anteriorly placed craniomandibular joint¹³. The prootic also has an anterior contact with a plate-like ossification of the primary braincase wall (Extended Data

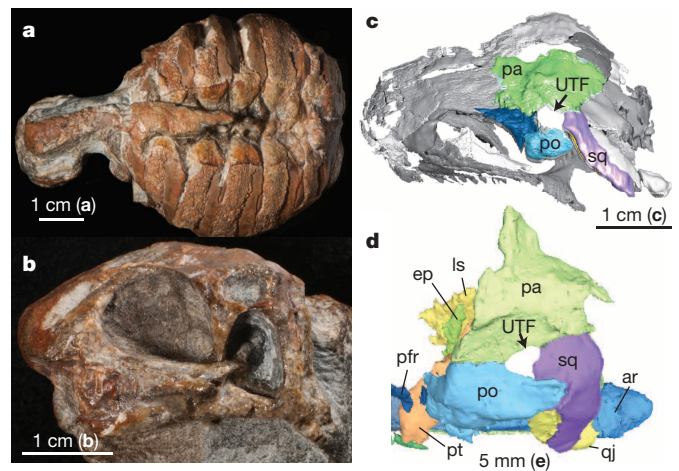


Figure 3 | The body plan of the early stem turtle *Eunotosaurus africanus*. a, b, The postcranium (a) and skull (b) of a juvenile *Eunotosaurus africanus* (SAM-PK-K7909) in dorsal and right lateral (reflected) views, respectively. c, d, The digitally rendered adult skull of *Eunotosaurus* in dorsolateral (CM777; c) and dorsal (CM86–341; d) views, with the supratemporal bone digitally removed in each. The UTF, clearly expressed in the juvenile, is retained in the adult but covered by the postnatal development of an elongate supratemporal bone. The size of the UTF and LTF of adult *Eunotosaurus* is reduced through late-stage ontogenetic expansion of the surrounding dermal elements. Abbreviations as in Figs 1 and 2. Scale bars: a–c, 1 cm; d, 5 mm.

Figs 1 and 3) that corresponds to a rare combination of ossified orbital cartilages present at least in *Proganochelys quenstedti* among stem turtles²¹.

These data resolve the cranial–postcranial conflict in that both modules now support *Eunotosaurus* as an early stem turtle, thus bolstering evidence for the turtle stem in the terrestrial ecosystem of Gondwana approximately 260 million years ago (Supplementary Tables 1–3). Considering that *Eunotosaurus* is widely accepted as lying outside the pandiapsid radiation, this shared signal seems only to exacerbate the phylogenetic gap between the phenotypic and genotypic explanations of turtle origins. Although it is the case that neither our parsimony nor Bayesian analyses recover the dominant molecular solution of a unique turtle–archosaur relationship, both approaches do agree that turtles arose somewhere within the greater diapsid radiation (Extended Data Figs 4 and 5). Our morphological results remain ambiguous as to whether that origin is nested within the diapsid crown clade or among those stem forms expressing a morphologically diapsid skull. The lack of clear morphological support for the refined position of turtles within Eureptilia probably reflects some combination of the rate at which these stem lineages diversified and our poor understanding of their respective fossil records²². For example, the early lepidosaur stem comprises comparatively few taxa, and the most conservative stem archosaurs bear a striking resemblance to apparent proximal stem diapsids, throwing into question the sequence of acquisition and degree of variability of crown diapsid autapomorphies²³.

The presence of a lower temporal fenestra in *Eunotosaurus* supports the hypothesis that the characteristically closed cheek of modern turtles is a secondary condition that evolved through expansion of the jugal, quadratojugal, and squamosal²⁴. Singular expression of a lower temporal fenestra once unambiguously diagnosed mammals and their stem lineage¹⁰ but is now recognized in a number of phylogenetically disparate ‘anapsid’ parareptiles²⁵, and may represent the ancestral condition for the amniote crown²⁶. This observed pattern of concentrated homoplasy near the evolutionary origin of a character state is congruent with the concept of a protracted zone of variability that may commonly confound attempts to resolve the early history of clades and character systems²⁷.

The amniote upper temporal fenestra has enjoyed a famously uncomplicated history, being a nearly consistent fixture of the diapsid body plan since its first appearance in the Carboniferous²⁸. The combined morphologies expressed in the juvenile and adult specimens of

Eunotosaurus provide not only the earliest direct evidence of an upper temporal fenestra in a putative stem turtle, but the first evidence for how that fenestra may have closed before the origin of the turtle crown clade. This evidence supports a model of temporal closure whose initial steps include a significant expansion of the dermal roof (postorbital, squamosal, and probably parietal) that first constricts and then closes the upper temporal fenestra (Fig. 4). Such steps are expected components of any hypothesis where turtles evolve from a diapsid ancestor. The addition of *Eunotosaurus* to this model is significant because it provides the first empirical evidence of these transitional expansions, which in turn allows the timing of these transformations to be anchored within the geological history of diapsids. *Eunotosaurus* also provides insight into the possible role of developmental timing in producing the modern anapsid condition. Phylogenetic acceleration (peramorphosis) of the inferred postnatal trajectory of dermal expansion around the temporal fenestrae of *Eunotosaurus* may explain the transition from a *Eunotosaurus*-like morphology to that expressed in *Odontochelys*, *Proganochelys*, and more crown-ward turtles.

The role of the supratemporal is an aspect of the *Eunotosaurus* model of temporal closure that would not have been predicted based on earlier studies. An anteriorly expanded supratemporal that develops late in postnatal development to cover the upper temporal fenestra must currently be considered an autapomorphy of *Eunotosaurus*. Future fossil discoveries will determine whether an expanded supratemporal was ancestral to crown-ward turtles, but it is important to stress that an expanded supratemporal is not a necessary component of an evolutionary model of fenestral closure in turtles that has *Eunotosaurus* as a central figure. For example, an analogous secondary expansion of the supratemporal partially or completely covers the upper temporal fenestra of the marine thalattosaurs²⁹. Moreover, the construction of the modern turtle skull played out over a time span of tens of millions of years, and it is well attested that dermal bones in major vertebrate lineages can shift back and forth considerably relative to the underlying tissues on these timescales; for instance in the complex history of the synapsid skull and the shoulder girdle of sarcopterygians (and tetrapods, most notably turtles themselves³⁰).

It is thus evident that the turtle skull, like the turtle postcranium, underwent profound modifications during its history that similarly obscured anatomical evidence for phylogenetic affinities by the time the crown-group condition was reached. The ecological context in which the earliest stem turtles lost their upper temporal fenestra is

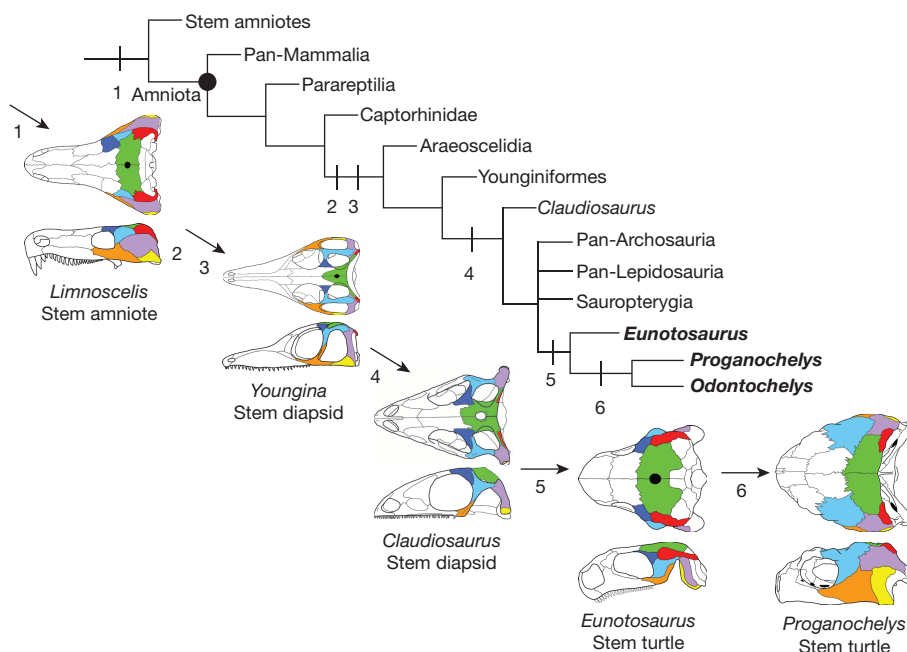


Figure 4 | Generalized amniote phylogeny showing sequence of major transformations in the origin of the turtle skull. (1) Ancestral crown amniote retains anapsid condition of amniote stem. (2) and (3) LTF and UTF appear, producing a fully diapsid skull. (4) Loss of lower temporal bar results in ventrally open LTF. (5) Size of UTF and LTF constricted through postnatal expansion of surrounding dermal elements (most notably postorbital and squamosal). Superficial covering of the UTF by the supratemporal, as expressed in *Eunotosaurus*, may or may not be ancestral to modern turtles. (6) Closure of LTF and UTF, perhaps involving a peramorphic shift in dermal bone growth. A secondary reduction of the supratemporal also may have occurred at this point.

unclear, although the upper fenestra in extant diapsids relates to the bulging of the pseudotemporalis muscle mass. It is thus likely that fenestral closure along the turtle stem had implications for the masticatory apparatus, and these implications may be reflected in the various modifications of the rostral portion of the skull.

Online Content Methods, along with any additional Extended Data display items and Source Data, are available in the online version of the paper; references unique to these sections appear only in the online paper.

Received 28 April; accepted 3 July 2015.

Published online 2 September 2015.

- Li, C., Wu, X.-C., Rieppel, O., Wang, L.-T. & Zhao, L.-J. An ancestral turtle from the Late Triassic of southwestern China. *Nature* **456**, 497–501 (2008).
- Lyson, T. R., Bever, G. S., Bhullar, B.-A. S., Joyce, W. G. & Gauthier, J. A. Transitional fossils and the origin of turtles. *Biol. Lett.* **6**, 830–833 (2010).
- Lyson, T. R., Bever, G. S., Scheyer, T. M., Hsiang, A. Y. & Gauthier, J. A. Evolutionary origin of the turtle shell. *Curr. Biol.* **23**, 1113–1119 (2013).
- Lyson, T. R. *et al.* Origin of the unique ventilatory apparatus of turtles. *Nat. Commun.* **5**, 5211 (2014).
- Schoch, R. R. & Sues, H.-D. A Middle Triassic stem-turtle and the evolution of the turtle body plan. *Nature* **523**, 584–587 (2015).
- Wang, Z. *et al.* The draft genomes of soft-shell turtle and green sea turtle yield insights into the development and evolution of the turtle-specific body plan. *Nature Genet.* **45**, 701–706 (2013).
- Field, D. J. *et al.* Toward concision in reptile phylogeny: miRNAs support an archosaur, not lepidosaur, affinity for turtles. *Evol. Dev.* **16**, 189–196 (2014).
- Joyce, W. G. & Gauthier, J. A. Palaeoecology of Triassic stem turtles sheds new light on turtle origins. *Proc. R. Soc. Lond. B* **271**, 1–5 (2004).
- Scheyer, T. M. & Sander, P. M. Shell bone histology indicates terrestrial palaeoecology of basal turtles. *Proc. R. Soc. Lond. B* **274**, 1885–1893 (2007).
- Gauthier, J., Kluge, A. G. & Rowe, T. Amniote phylogeny and the importance of fossils. *Cladistics* **4**, 105–209 (1988).
- Cundall, D. & Irish, F. in *Biology of the Reptilia* Vol. 20 (eds Gans, C., Gaunt, A. S., Adler, K.) 349–692 (Society for the Study of Amphibians and Reptiles, 2008).
- Bhullar, B.-A. S. *et al.* Birds have paedomorphic dinosaur skulls. *Nature* **487**, 223–226 (2013).
- Gaffney, E. S. The comparative osteology of the Triassic turtle *Proganochelys*. *Bull. Am. Mus. Nat. Hist.* **194**, 1–263 (1990).
- Werneberg, I. Temporal bone arrangements in turtles: an overview. *J. Exp. Zool. B* **318**, 235–249 (2012).
- Müller, J. in *Recent Advances in the Origin and Early Radiation of Vertebrates* (eds Arratia, G., Wilson, M. V. H., Wilson, R., Cloutier, R.) 379–408 (Verlag Dr. Friedrich Pfeil, 2004).
- Lee, M. S. Y. Turtle origins: insights from phylogenetic retrofitting and molecular scaffolds. *J. Evol. Biol.* **26**, 2729–2738 (2013).
- Day, M., Rubidge, B., Almond, J. & Sifelani, J. Biostratigraphic correlation in the Karoo: the case of the Middle Permian parareptile *Eunotosaurus*: research letter. *S. Afr. J. Sci.* **109**, 1–4 (2013).
- Cox, C. B. The problematic Permian reptile *Eunotosaurus*. *Bull. Br. Mus. Nat. Hist.* **18**, 165–196 (1969).
- Keyser, A. W. & Gow, C. E. First complete skull of the Permian reptile *Eunotosaurus africanus* Seeley. *S. Afr. J. Sci.* **77**, 417–420 (1981).
- Gow, C. E. A reassessment of *Eunotosaurus africanus* Seeley (Amniota: Parareptilia). *Palaeont. Afr.* **34**, 33–42 (1997).
- Bhullar, B.-A. S. & Bever, G. S. An archosaur-like laterosphenoid in early turtles (Reptilia: Pantestudines). *Breviora* **518**, 1–11 (2009).
- Reisz, R. R., Modesto, S. P. & Scott, D. M. A new Early Permian reptile and its significance in early diapsid evolution. *Proc. R. Soc. Lond. B* **278**, 3731–3737 (2011).
- Bickelmann, C., Müller, J. & Reisz, R. R. The enigmatic diapsid *Acerosodontosaurus piveteaui* (Reptilia: Neodiapsida) from the Upper Permian of Madagascar and the paraphyly of “younginiform” reptiles. *Can. J. Earth Sci.* **46**, 651–661 (2009).
- Müller, J. Early loss and multiple return of the lower temporal arcade in diapsid reptiles. *Naturwissenschaften* **90**, 473–476 (2003).
- Tsuji, L. A. & Müller, J. Assembling the history of the Parareptilia: phylogeny, diversification, and a new definition of the clade. *Fossil Rec.* **12**, 71–81 (2009).
- Piñero, G., Ferigolo, J., Ramos, A. & Laurin, M. Cranial morphology of the Early Permian mesosaurid *Mesosaurus tenuidens* and the evolution of the lower temporal fenestration reassessed. *C. R. Palevol* **11**, 379–391 (2012).
- Bever, G. S., Gauthier, J. A. & Wagner, G. P. Finding the frame shift: digit loss, developmental variability, and the origin of the avian hand. *Evol. Dev.* **13**, 269–279 (2011).
- Reisz, R. R. *A Diapsid Reptile from the Pennsylvanian of Kansas* (Univ. of Kansas, 1981).
- Rieppel, O. *Clarazia* and *Hescheleria*: a re-investigation of two problematical reptiles from the Middle Triassic of Monte San Giorgio (Switzerland). *Palaeontogr. Abt. A* **195**, 101–129 (1987).
- Lyson, T. R. *et al.* Homology of the enigmatic nuchal bone reveals novel reorganization of the shoulder girdle in the evolution of the turtle shell. *Evol. Dev.* **15**, 1–9 (2013).

Supplementary Information is available in the online version of the paper.

Acknowledgements We thank J. Botha-Brink, E. Butler, S. Kaal, E. De Kock, J. Neveling and R. Smith for access to *Eunotosaurus* specimens. M. Fox and Z. Erasmus prepared fossil material. M. Colbert, J. Maisano, M. Hill and J. Thostenson are acknowledged for their help with the digital data. We thank A. Balanoff, D. Dykes, J. Gauthier, R. Hill, B. Rubidge, R. Smith and K. de Queiroz for helpful discussions. G.S.B. extends special thanks to the Academic Technologies Group at NYIT for their support in the digital visualization of anatomical data.

Author Contributions G.S.B. designed the study, processed the CT data, performed the analytical work, constructed the figures, and wrote the paper. T.R.L. performed analytical work, assisted writing the paper, and assisted with figures. D.J.F. and B.-A.S.B. performed analytical work and assisted writing the paper.

Author Information Reprints and permissions information is available at www.nature.com/reprints. The authors declare no competing financial interests. Readers are welcome to comment on the online version of the paper. Correspondence and requests for materials should be addressed to G.S.B. (gbever@nyit.edu).

METHODS

No statistical methods were used to predetermine sample size. The experiments were not randomized and the investigators were not blinded to allocation during experiments and outcome assessment.

Specimens and CT scanning. Although *Eunotosaurus africanus* is known from a surprisingly large number of specimens ($n > 44$), relatively few of these include cranial material (see below). Our study was built largely around the adult morphology of CM777 and CM86-341, and the juvenile features of SAM-PK-K7909. NMQR3299 was also examined, but relatively poor preservation restricted its contribution to our cranial assessments. The skull of CM 777 was scanned at the University of Texas High-Resolution X-ray CT Facility (UTCT). Scanning was performed using no filter, an air wedge, a voltage of 200 kV and a current of 0.17 mA. The resulting images were then processed for the removal of ring artefacts. The specimen was scanned along the coronal axis for a total of 1,003 slices with an image resolution of 1024×1024 pixels and a reconstructed field of view of 34 mm. Voxel size (mm) is $0.03657 \times 0.03320 \times 0.03320$. Each image has a reconstructed field of view of 34 mm. Additional images are available at DigiMorph (http://www.digimorph.org/specimens/Eunotosaurus_africanus). Original slice data are available on request.

NMQR3299 (skull and postcranial skeleton) was scanned at UTCT with no filter, an air wedge, a voltage of 200 kV, and a current of 0.19 mA. Ring artefacts were removed. Scanning was performed along the coronal axis for a total of 1,764 slices with a resolution of 1024×1024 pixels and a reconstructed field of view of 62 mm. Voxel size (mm) is $0.06065 \times 0.06065 \times 0.06618$. No digital segmentation of this data set was performed.

CM86-341 was scanned at the American Museum of Natural History Microscopy and Imaging Facility (AMNH MIF) using a copper filter, an air wedge, a voltage of 150 kV, and a current of 124 mA. The specimen was scanned along the coronal axis for a total of 950 slices with a resolution of 1024×1024 pixels and a reconstructed field of view of 35 mm. Voxel size (mm) is $0.03403 \times 0.03403 \times 0.03403$. Digital segmentation of the recognizable cranial elements was performed using VGStudioMax2.1.

This study also includes novel morphological data derived from the recent physical preparation of two specimens of *Eunotosaurus* (using small PaleoTools microjack and microscope). CM86-341 was prepared in 2010–2012 by M. Fox (Peabody Museum, Yale University) under the direction of J. Gauthier. SAM-PK-K7670 was prepared in 2014–2015 by Z. Erasmus (Iziko Museums of South Africa) under the direction of R. Smith.

List of examined cranial specimens of *Eunotosaurus africanus*. CM86-341: beautifully preserved partial skull, completely articulated neck with a few cervical ribs, and complete carapace (nine dorsal vertebrae and nine pairs of dorsal ribs) (Fig. 2 and Extended Data Fig. 1). CM777: articulated skull, neck, elongate cervical ribs, shoulder girdle, limb elements, and cranial half of carapace including dorsal vertebrae and ribs (Fig. 2 and Extended Data Figs 2 and 3). Unnumbered CM specimen figured in ref. 19. NMQR3299: mostly complete skeleton including articulated skull (Fig. 2). NMQR3474: impression of a mostly articulated skeleton, including the skull. SAM-PK-K7670: highly weathered nodule with mostly complete skeleton including cranial two-thirds dorsal ribs and vertebrae, impressions of the cervical vertebrae, and an impression of the skull. SAM-PK-K7909: weathered nodule with complete shell and shoulder girdle, articulated neck, and essentially complete and articulated skull (Fig. 3). Juvenile based on its small size and expression of numerous features indicative of skeletal immaturity in reptiles (that is, unfused scapula and coracoid)^{31,32}.

Institutional abbreviations used are as follows: CM, Council for Geosciences, Pretoria; NMQR, National Museum, Bloemfontein; RC, Rubidge Collection, Graaff-Reinet; SAM-PK, Iziko Museums of South Africa, Cape Town; YPM, Peabody Museum, Yale University, New Haven.

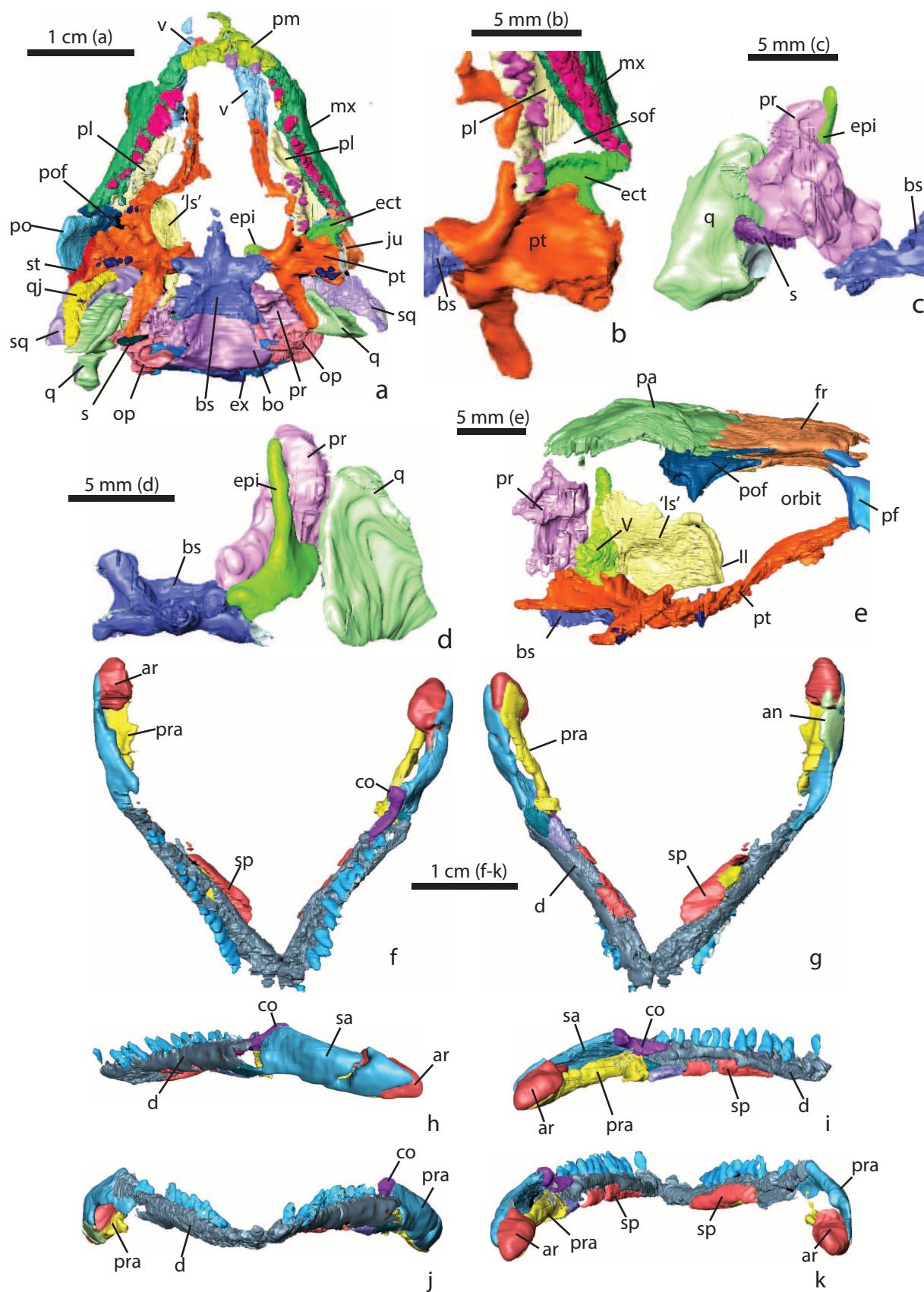
Phylogenetic analysis. The phylogenetic relationships of *Eunotosaurus africanus* were assessed using a novel character/taxon matrix consisting of 268 characters (174 cranial, 94 postcranial) scored for 47 taxa distributed broadly across amniotes with emphasis on Pan-Reptilia. Our primary purpose was to determine how an enhanced understanding of the cranial anatomy of *Eunotosaurus* affects its phylogenetic status as an early stem turtle and the topological position of turtles in general. This is especially important considering that many of the more compelling *Eunotosaurus*–turtle synapomorphies are features associated with the iconic, shelled body plan^{2–4}. While of considerable interest, the shared expression of these features also raises the question of convergence—perhaps there are only so many ways to build a shell. The skull serves as a relatively independent module on which to test the *Eunotosaurus*–turtle hypothesis.

Tree topologies were inferred using both maximum parsimony and Bayesian optimality criteria. To specifically assess the dominant phylogenetic signal within the cranial data, separate analyses were performed on the complete matrix and a matrix restricted to cranial characters. The maximum parsimony tree was generated using TNT1.1³³. *Seymouria* spp. was specified as the outgroup, and heuristic searches were conducted using tree-bisection-reconnection (TBR) branch swapping with 1,000 replicates of random stepwise sequence addition. Minimum branch lengths were set to collapse. Support for each node was measured by calculating Bremer support and bootstrap frequencies, with 1,000 bootstrap replicates and 1,000 random sequence addition replicates. Characters 34, 62, 67, 85, 107, 118, 148, 155, 193 and 220 (Supplementary Table 1) were treated as ordered as their derived states were interpreted as non-mutually exclusive (that is, the possession of either derived state reflects shared information that should be considered in the analysis). The implications of this approach were tested by comparing the results with iterations where all characters were analysed as unordered.

Bayesian phylogenetic analyses were run using MrBayes (v3.2.2)³⁴ on the CIPRES Science Gateway³⁵. The Mk model³⁶ was used to analyse the full and cranial-only character matrices with gamma-distributed rate variation and variable coding. All analyses were performed with a sampling frequency of 1,000, two concurrent runs, and four Metropolis-coupled chains ($T = 0.1$) for 30,000,000 generations. Characters 34, 62, 67, 85, 107, 118, 148, 155, 193 and 220 were again treated as ordered. All analyses were checked for convergence using standard MrBayes diagnostics (for example, PRSF < 0.01, mixing between chains > 20%) and Tracer (v1.5)³⁷ (for example, ESS > 200). A 25% relative burn-in was implemented for all summary statistics.

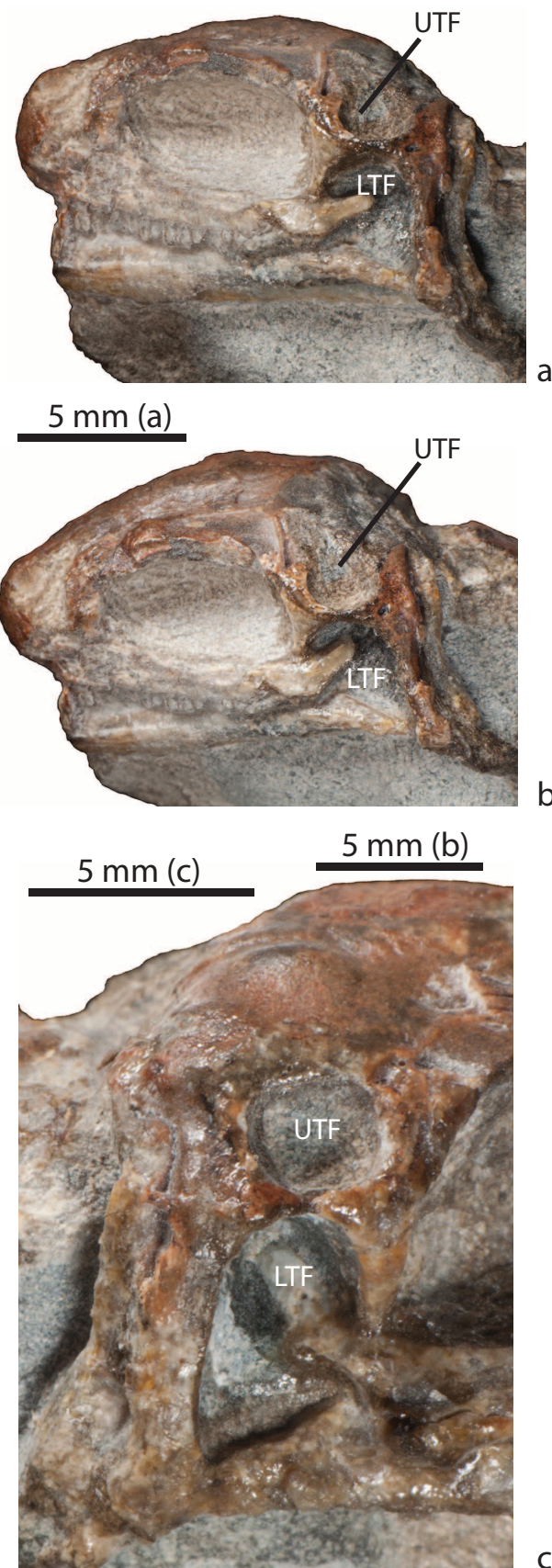
A list of the cranial characters and their definitions is provided as Supplementary Table 1. Postcranial characters are taken directly from ref. 3. Supplementary Table 2 provides character scores and Supplementary Table 3 provides a list of synapomorphies for each of the reptile clades within which *Eunotosaurus* is nested. Supplementary Table 4 lists the observed specimens and primary references from which we compiled our character matrix.

31. Romer, A. S. *Osteology of the Reptiles* (Univ. Chicago Press, 1956).
32. Maisano, J. A. Terminal fusions of skeletal elements as indicators of maturity in squamate reptiles. *J. Vertebr. Paleontol.* **22**, 268–275 (2002).
33. Goloboff, P. A., Farris, J. & Nixon, K. TNT: a free program for phylogenetic analysis. *Cladistics* **24**, 774–786 (2008).
34. Ronquist, F. & Huelsenbeck, J. P. MRBAYES 3: Bayesian phylogenetic inference under mixed models. *Bioinformatics* **19**, 1572–1574 (2003).
35. Miller, M. A., Pfeiffer, W. & Schwartz, T. in *Proceedings of the Gateway Computing Environments Workshop* 1–8 (IEEE, 2010).
36. Lewis, P. O. A likelihood approach to estimating phylogeny from discrete morphological character data. *Syst. Biol.* **50**, 913–925 (2001).
37. Drummond, A. J., Suchard, M. A., Xie, D. & Rambaut, A. Bayesian phylogenetics with BEAUti and the BEAST 1.7. *Mol. Biol. Evol.* **29**, 1969–1973 (2012).



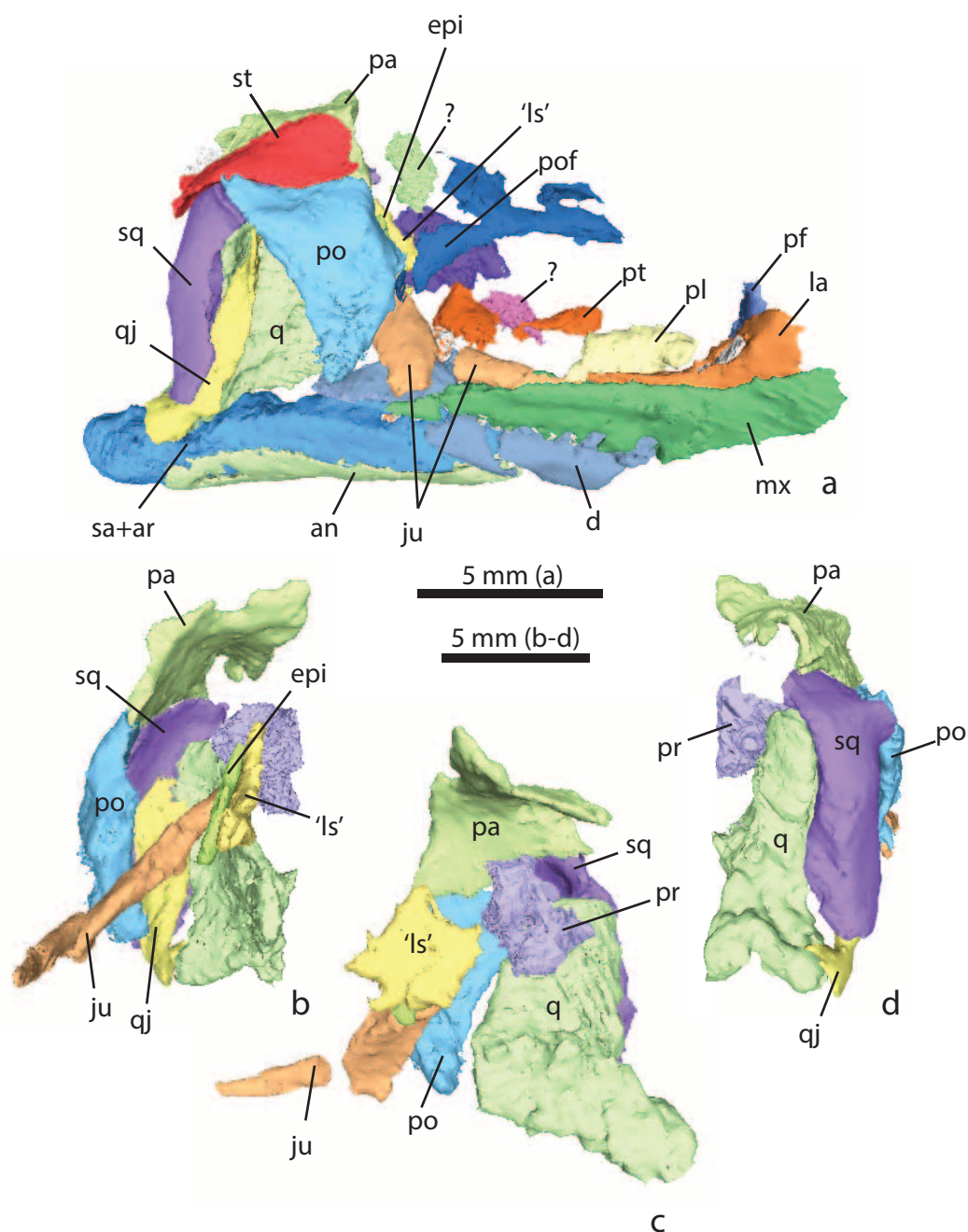
Extended Data Figure 1 | Digital reconstruction of segmented cranial elements of *Eunotosaurus africanus* CM 777. **a**, Palatal view with the lower jaws digitally removed and major roofing elements not rendered. **b**, Anteromedial view of left palate showing moderately sized suborbital fenestra. **c**, **d**, Posteromedial (**c**) and anterolateral (**d**) views of left quadrate, prootic, stapes, epipterygoid and midline parabasisphenoid. **e**, Right lateral view of anterior braincase wall and surrounding elements. Note sutural contact of prootic and quadrate. **f–k**, Lower jaws in dorsal (**f**), ventral (**g**), left lateral (**h**),

medial (left jaw) (**i**), anterior (**j**), and posterior (**k**) views. an, angular; ar, articular; bs, parabasisphenoid; co, coronoid; d, dentary; ect, ectopterygoid; epi, epipterygoid; fr, frontal; ju, jugal; la, lacrimal; ls, laterosphenoid; mx, maxilla; op, opisthotic; pa, parietal; pf, prefrontal; pl, palatine; pm, premaxilla; po, postorbital; pof, postfrontal; pr, prootic; pra, prearticular; pt, pterygoid; q, quadrate; qj, quadratojugal; s, stapes; sq, squamosal; sof, suborbital fenestra; sp., splenial; st, supratemporal; sa, surangular; v, vomer; IL, inferred exit point for orbital nerve; V, prootic incisure, exit point for trigeminal nerve.



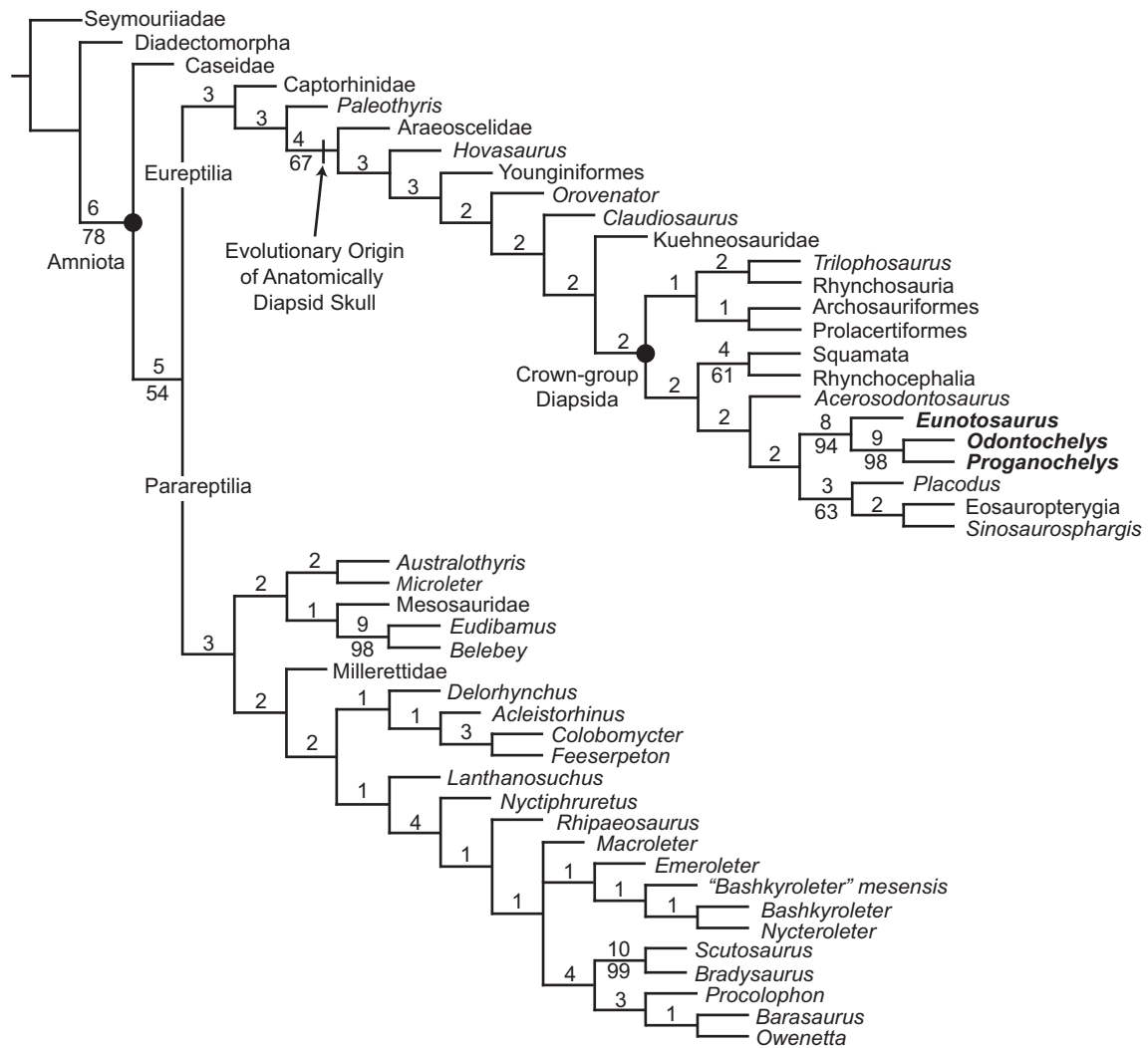
Extended Data Figure 2 | The juvenile skull of *Eunotosaurus africanus* (SAM-PK-K7909) showing clear expression of both LTF and UTF. a, b, Left lateral view with the rostrum held horizontally (a) and slightly downturned (b). c, Close-up view of fenestrated cheek in right lateral view. The size of the

fenestrae decreases in the late stages of postnatal ontogeny through expansion of the surrounding dermal bones. The upper temporal fenestra is eventually obscured by the late-stage ontogenetic development of an elongate supratemporal.



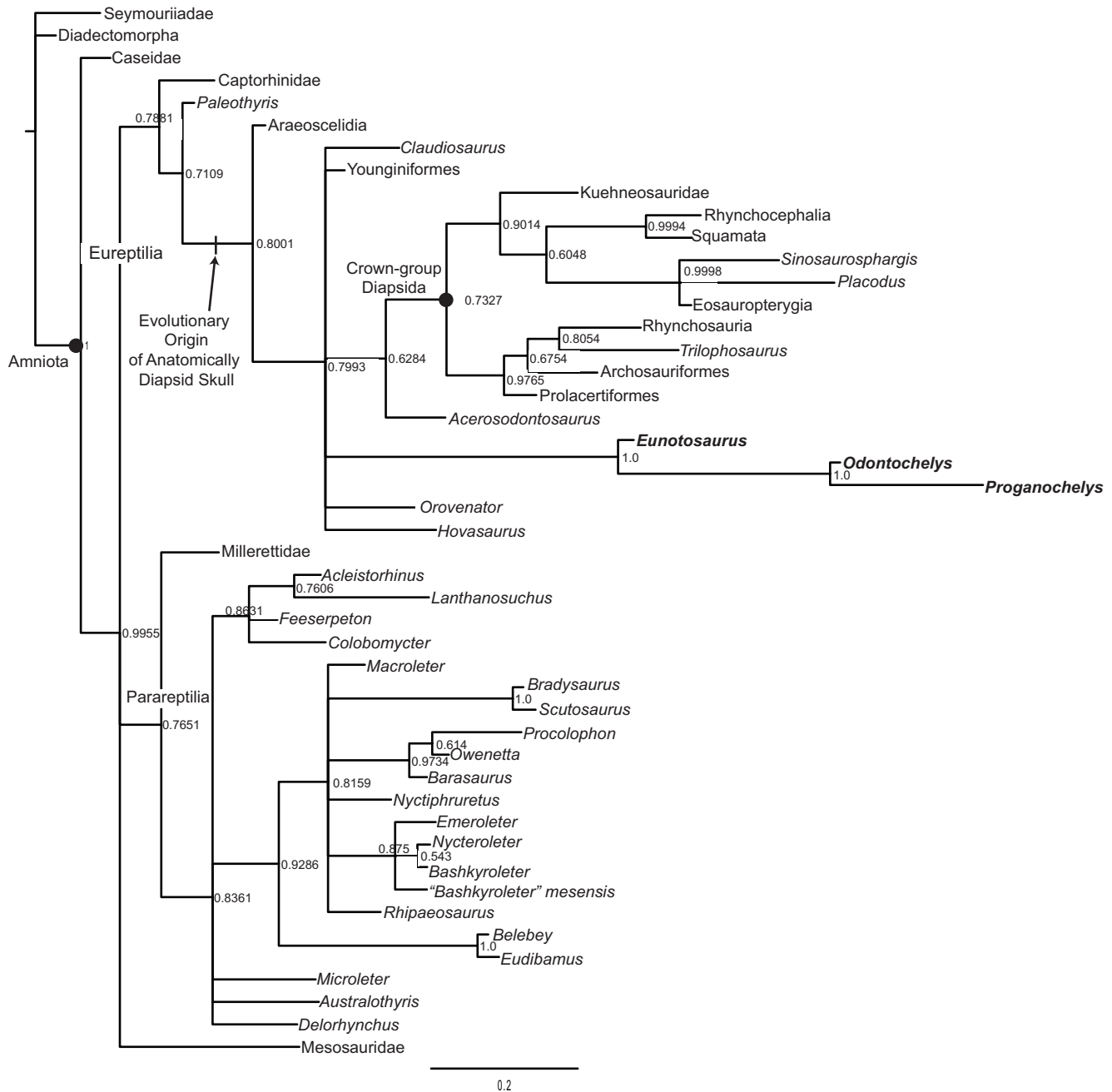
Extended Data Figure 3 | Digitally segmented and reconstructed cranial elements of *Eunotosaurus africanus* (CM86-341). a–d, Right lateral view (a), anterior (b), posterior (c), and right medial (d) views. an, angular; d, dentary; epi, epipterygoid; ju, jugal; la, lacrimal; 'ls', 'laterosphenoid'; mx,

maxilla; pa, parietal; pf, prefrontal; pl, palatine; po, postorbital; pof, postfrontal; pt, pterygoid; q, quadrate; qj, quadratojugal; sa + ar, surangular and articular; sq, squamosal; st, supratemporal; UTF, upper temporal fenestra; ?, unclear identity.



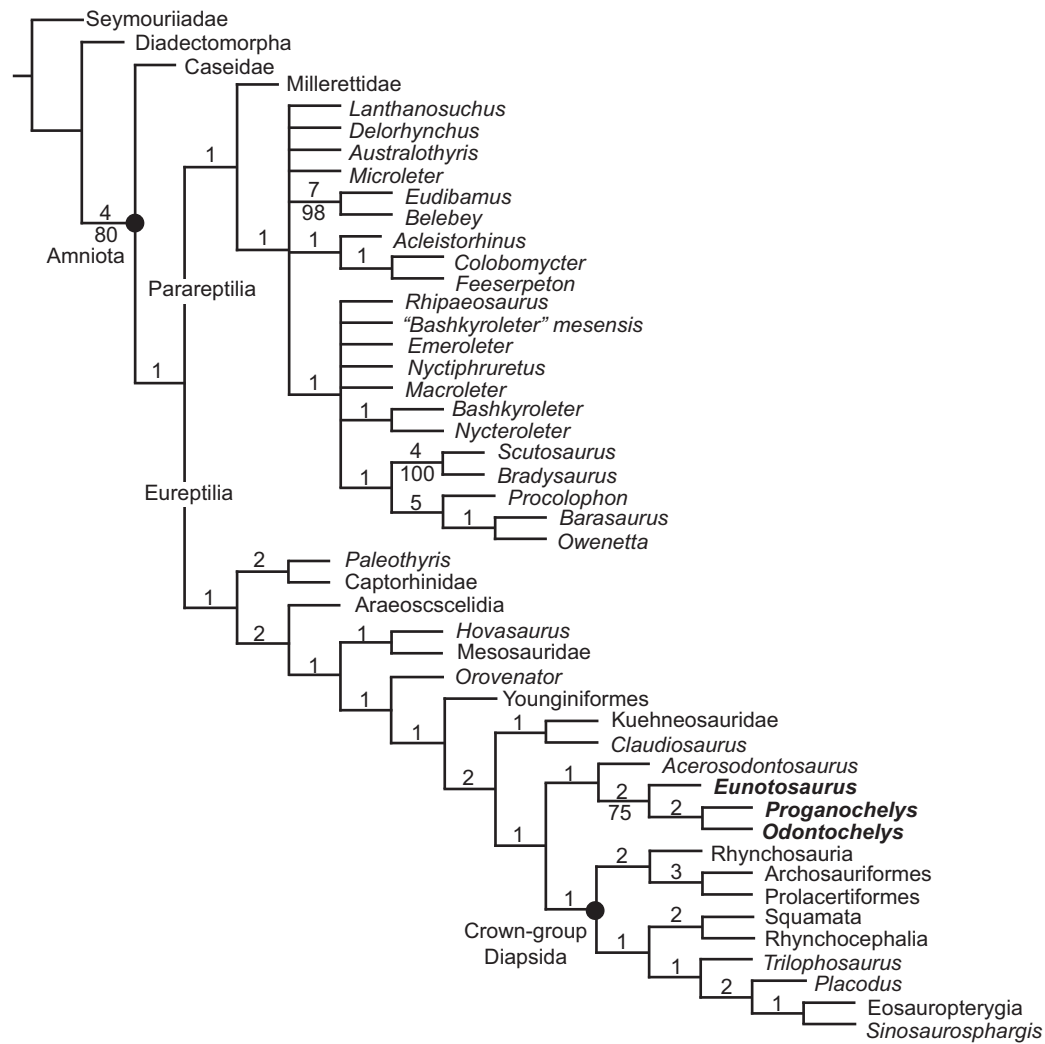
Extended Data Figure 4 | Strict consensus of two most parsimonious recovered from total character matrix. Bremer support values are provided for each clade (above line). Bootstrap values exceeding 50% are provided (below line). A *Eunotosaurus*–turtle clade is extremely well supported. That this

pan-turtle lineage originated somewhere within the radiation of anatomically diapsid reptiles is well supported, although a refined phylogenetic position remains morphologically elusive. Tree length = 1,087; consistency index = 0.4013; retention index = 0.590.



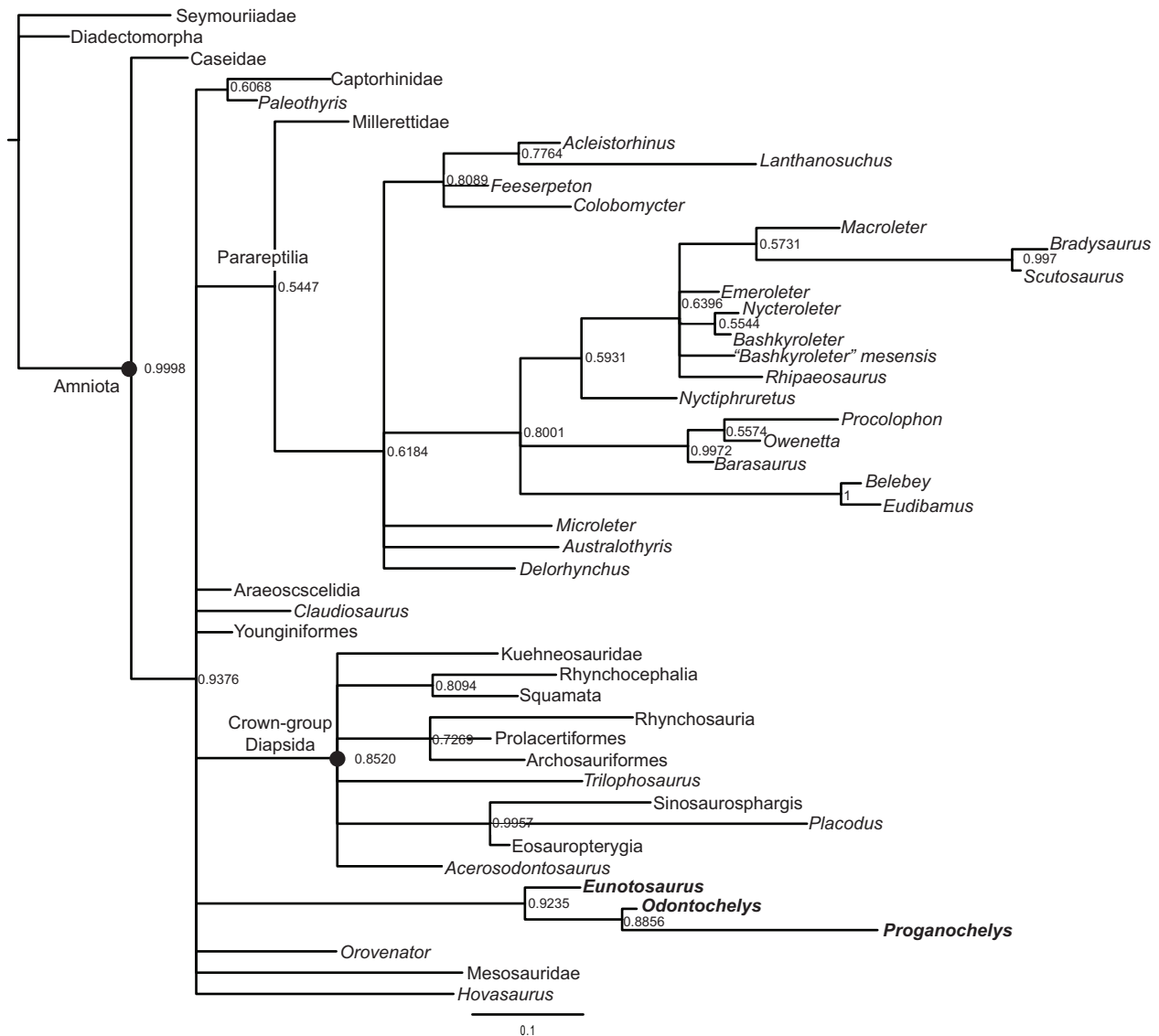
Extended Data Figure 5 | Bayesian tree topology derived from total matrix (50% majority rule consensus). An exclusive *Eunotosaurus*–turtle clade is recovered with 100% posterior probability. This pan-turtle lineage is nested within the radiation of anatomically diapsid reptiles; however, in contrast to the parsimony solution, turtles are excluded from crown-group Diapsida. The

Bayesian results agree with the parsimony in revealing strong support that: (1) *Eunotosaurus* is an early stem-group turtle; and (2) the ancestral stem turtle expressed a fully diapsid skull. The two analyses also agree that there is currently poor morphological support for a refined position of turtles within the greater diapsid radiation.



Extended Data Figure 6 | Strict consensus of 13 most parsimonious trees recovered from cranial-only matrix. The *Eunosaurus*–turtle clade is recovered, which supports the hypothesis that the postcranial synapomorphies

of *Eunosaurus* and turtles are homologous and not the products of convergence. Tree length = 777; consistency index = 0.3956; retention index = 0.4743.



Extended Data Figure 7 | Bayesian tree topology derived from cranial-only matrix (50% majority rule consensus). When studied in isolation, cranial anatomy provides poor resolution of the deep divergences within Pan-Reptilia, but a *Eunotosaurus*–turtle signal is clearly present.